# All-Optical Preparation of Molecular Ions in the Rovibrational Ground State

T. Schneider, B. Roth, H. Duncker, I. Ernsting, S. Schiller

Institut für Experimentalphysik, Heinrich-Heine-Universität Düsseldorf, 40225 Düsseldorf, Germany

Version 1, submitted Aug. 30, 2009

Revised version 2 accepted for publication in Nature Physics

(see published article for final version that contains additional simulation results in the "Supplementary Materials")

## Introductory Paragraph

In the field of cold quantum matter, laser-based cooling of the motional degrees of freedom of gas phase molecules has been achieved for several neutral diatomic species, and many positively charged diatomic and polyatomic species [1] [2] [3] [4] [5] [6] [7] [8] [9] [10] [11]. However, laser cooling of the internal degrees of freedom has been challenging. Recently, transfer to the internal ground state by sophisticated optical techniques has been demonstrated for neutral alkali dimer created in single quantum states from ultracold atoms [12],[13],[14],[15]. Here we demonstrate cooling of the rotational degree of freedom of heteronuclear diatomic molecules with a thermal distribution of internal states, using a simple, robust, and general optical pumping scheme with two low-power continuous-wave lasers. With trapped and translationally sympathetically cooled $HD^+$ molecular ions as a model system, we achieve 78(4)% ro-vibrational ground state population. The rotationally, vibrationally, and translationally cold molecular ion ensemble is suitable for a number of applications, such as generation of long-lived coherences, systems with dipolar interactions [16], and frequency metrology of fundamental constants [17][18].

## Main text

The study of cold molecular systems promises new insights and advances in many fields of physics and physical chemistry. As in atomic physics the key to tapping the full potential of molecules is the ability to accurately control the external and internal degrees of freedom of the particles. The complex internal structure of molecules has however so far precluded direct application of many techniques developed for trapping and cooling of atoms, demanding modified or completely new approaches. By now, a large toolbox for trapping and cooling the motional degrees of freedom of both neutral and charged molecules is available [19]. While general schemes for cooling the internal degrees of freedom of molecules have been proposed [20],[21], the most general method currently available is cryogenic buffer gas cooling which is efficient only for molecules in the vibrational ground state and limits the translational temperature to a few hundred milli-Kelvin [8]. Coherent transfer to the ro-vibrational ground state [12],[13],[14],[15] is most suitable when most of the molecules are initially in the same quantum state, as is the case for molecules produced by associating cold atoms.

For heteronuclear molecular ensembles whose population is distributed among many rotational levels in the $v = 0$ vibrational manifold, optical pumping has been proposed as an approach to rotational cooling [22][23]. We demonstrate here that a scheme using two laser fields driving a fundamental and an overtone vibrational electric dipole transition [22] yields a large ground-state population. The applicability to various molecular species is analyzed theoretically. The scheme's

relative simplicity is enhanced by using recently developed room-temperature cw mid-infrared diode lasers.

Fig. 1 shows the energy levels (without hyperfine structure) and electric dipole transitions of the $HD^+$ molecules relevant for the experiment. The initial internal state distribution is given by a Boltzmann distribution reflecting thermal equilibrium with the $T \cong 300$ K blackbody radiation field emitted by the experimental apparatus. For $HD^+$ this means that all of the ions are in the $v = 0$ vibrational state of the $1s\sigma$ electronic ground state, but only 10% are in the $(v = 0, J = 0)$ absolute rovibrational ground state. The remaining population is distributed mostly among the states $(v = 0, J = 1 - 5)$ with a maximum of 27% residing in the $(v = 0, J = 2)$ - state [24].

The set $\{(0,0),(0,1),(0,2),(1,1),(2,0)\}$ of rovibrational states (v, J) forms a nearly closed 5-level system with the rovibrational ground state as a dark state when interacting with two laser fields driving the $(0, 1)\rightarrow(2, 0)$ and $(0, 2)\rightarrow(1, 1)$ transitions. This leads to rapid optical pumping of the populations in $(0, J = 1, 2)$ to the (0, 0)-ground state. If the optical pump rates sufficiently exceed the rates at which the blackbody radiation redistributes the populations among rotational states, also most of the population in $(0, J > 2)$-states is transferred to the rovibrational ground state on a time scale given approximately by the inverse of the average blackbody redistribution rate. Since the spontaneous emission rates from the excited (2,0)- and (1,1)-states are large ($32\ s^{-1}$, $18\ s^{-1}$ ) compared to the blackbody redistribution rates ($< 1\ s^{-1}$), those conditions can be easily met and also redistribution among excited states by blackbody radiation is negligible. The maximum achievable steady-state population in the ground state is then limited by thermal excitation away from the ground state on the $(0, 0) \rightarrow (0, 1)$ transition, with rate $\Gamma_0(T) \cong 0.086\ s^{-1}$.

We model the internal state dynamics by a set of rate equations, see Methods Section. Under optimum conditions an accumulation $p_0 \cong 92\%$ of the population in the rovibrational ground state is predicted to be reached within 30 s (see Fig.2). The steady-state population fraction $1 - p_0$ not residing in the ground state is predicted to scale as $\Gamma_0(T)/A_{vib}$, where $A_{vib}$ is the spontaneous emission rate for a vibrational decay $\Delta v = 1$ (see Methods Section). For many heteronuclear molecular ions this ratio is $<< 1$ at room temperature, here 0.015, so that a large fraction of the population is pumped to the ground state, $(1 - p_0 << 1)$.

When optical pumping is stopped, the ground state population $p_0$ decays exponentially with a time constant $\tau \cong \Gamma_0(T)^{-1} \cong 11$ s as the system evolves back to thermal equilibrium. During the first 100 ms $p_0$ changes by less than 1%. For most types of measurements this is sufficient time for any further desired manipulation of the ground state molecules.

We apply the optical state preparation scheme to ensembles of typically 100 $HD^+$ ions trapped together with about 2000 laser cooled atomic $Be^+$ ions in a linear radiofrequency quadrupole ion trap under conditions where the ions form a Coulomb crystal (for a detailed description of the experimental setup see [10],[24]). The laser-cooled $Be^+$ ions provide sympathetic translational cooling for the $HD^+$ ions to $T \lesssim 50$ mK and a means for detection of the molecules. We measure the rotational state distribution in the $v = 0$ state by a combination of resonant excitation of the

$HD^+$ ions' secular motion in the trap and rotational state selective (1+1') Resonance Enhanced Multi-Photon Dissociation (REMPD) [24] (see Methods Section).

For optical pumping we use two laser sources: a room-temperature cw quantum cascade laser (QCL) driving the (0, 2)→(1, 1) transition at 5484 nm ($I_{QCL} \cong 12$ μW/mm$^2$) that is continuously frequency referenced to an absorption line in $NH_3$ and spectrally broadened to 100 $MHz_{pp}$. The second laser is a cw distributed feedback (DFB) diode laser driving the (0, 1)→(2, 0) transition at 2713 nm ($I_{DFB} \cong 0.3$ mW/mm$^2$). During optical pumping the center frequency of the laser is not actively stabilized and the frequency spectrum is broadened to 200 $MHz_{pp}$ by current modulation. The rest of the time, the modulation is turned off and the laser is continuously frequency referenced to an absorption line in $CO_2$. For both the QCL and the DFB laser the intensity is larger than the saturation intensity of the respective transition.

The experimental sequence is shown in Fig. 3. We first load $HD^+$ ions into the trap. Then we resonantly excite the $HD^+$ ions' secular motion for $t_s = 5$ s to obtain the $Be^+$ fluorescence change $\langle\Delta\Gamma_1\rangle$ before we optically pump for $t_p = 40$ s with the QCL and DFB laser. After that we apply our REMPD-lasers for $t_d = 3$ s with the diode laser tuned to one of the (0, J)→(4, J+1) transitions. Finally we do another 5 s of secular excitation to obtain $\langle\Delta\Gamma_2\rangle$. For every state (0, J = 0 - 4) we repeat the sequence typically ten times and determine the average detection signal $\langle S_J\rangle = 1 - (\langle\Delta\Gamma_2\rangle/\langle\Delta\Gamma_1\rangle)$. The detection time was optimized by measuring $\langle S_0\rangle$ for successively increasing values of $t_d$ until $\langle S_0\rangle$ starts to level off.

Fig. 4 shows a measurement of the rotational state distribution for J = 0 - 4 together with the predictions of the rate equation calculations including the REMPD-detection for our experimental parameters. The background corrected detection signals $\langle S_{Jb}\rangle = \langle S_J\rangle - \langle S_b\rangle$ ($\langle S_b\rangle = 0.03(3)$) are determined from 18 (J = 0), 10 (J > 0), and 25 (background) individual measurements each. For the ground state we find $\langle S_{0b}\rangle = 0.78(4)$, which is 85% of the theoretical optimum $p_0 = 0.92$ and nearly a factor 8 larger than the thermal equilibrium population at room temperature. The simulation predicts an actual detection signal $S_0 = 0.89$ limited by the available power of the UV-dissociation laser. The above value therefore represents a lower bound on the actual ground state population. Comparing the ratios $R_J = \langle S_{Jb}\rangle/S_J$ of measured to predicted detection signals for states with a sizable population (J < 3) we find values $R_J = 0.8$-$0.9$. We also did measurements for variable optical pump times $t_p$ as well as for optical pumping with only the QCL or the DFB laser where we again find $R_J = 0.8$-$0.9$, confirming that the rate equation model presented above gives for the $HD^+$ molecule a good description of the internal state dynamics. We ascribe the small discrepancy between theory and experiment to the simplified treatment of the hyperfine structure in the simulations combined with a lower than calculated excitation rate on the (0, J)→(4, J+1) transitions used for REMPD-detection. The latter is evident from the unexpectedly long optimum detection time $t_d = 3$ s found in the experiment, which can only be explained by a reduced excitation rate on the (0,J)→(4,J+1) transition during detection. Possible contributions to this effect are an imperfect overlap between the diode laser focus and the ion ensemble and the unnecessarily large and currently not adjustable spectral broadening of the diode laser. The result

is a reduction of $S_0$ compared to the actual ground state population $p_0$ because $t_d$ is not sufficiently short compared to the blackbody thermalization time. For $J > 0$ on the other hand the simulations predict $S_J > p_J$ for the same reason in good agreement with the experimental data. For $J > 0$ our detection signals therefore give an upper bound for the actual state populations $p_J$.

In Fig. 4 we also compare the measured rotational state distribution to a Boltzmann distribution that gives the same ground state population $p_0$ resulting in an effective rotational temperature $T_{eff}$=26.5 K. While such a temperature could also be achieved using a cryogenic setup, the all-optical method has several advantages: it puts less constraints on the design of the experiment, is faster than waiting for thermalization with a cold environment and compared to cryogenic buffer gas cooling it does not compromise the translational temperature of the sample.

In conclusion, we have demonstrated an all-optical scheme for transferring vibrationally cold heteronuclear diatomic molecular ions, here $HD^+$ ions, to their rovibrational ground state, using optical pumping by two cw lasers. The measured ground state population of 0.78(4) represents a lower bound for the actual ground state population and is currently limited mainly by the efficiency of the employed detection. A high transfer efficiency is one of the main prerequisites for achieving a good signal to noise ratio in high precision spectroscopy, especially when ultimately experimenting with single molecular ions. A logical next step is to extend the rotational cooling by a 1.3 THz radiation source for addressing individual hyperfine components of the fundamental rotational transition $(0, 0)\rightarrow(0, 1)$. This will allow preparing the ions also in a specific hyperfine sub-level of the rovibrational ground state and enable precise measurements of the $HD^+$ hyperfine structure as well as improved absolute frequency measurements of rovibrational transition frequencies [18].

We expect that the two-laser optical pumping scheme can be applied also to many other heteronuclear diatomic molecules with comparable efficiency and simplicity.

# Methods

## Rate equation model

The rate equations for heteronuclear diatomics [Vogelius2] are based on Einstein A and B coefficients which for $HD^+$ are derived from theoretical values for transition energies [Korobov1] and transition dipole moments [Colbourn1]. The numerical model includes states (v = 0 - 4, J = 0 - 9) and interaction with the unpolarized blackbody radiation field as well as the linearly polarized laser fields for optical pumping and molecule detection. Rotational blackbody excitation and deexcitation is taken into account only in the v = 0 level. The neglect of such processes within v = 1, 2 compared to vibrational spontaneous emission to the v – 1 level requires that the ratio of the fundamental rotational frequency $\nu_{rot}$ and the blackbody temperature be sufficiently large, $\exp(h \nu_{rot}/k_B T) - 1 >> 2 A_{11,10}/A_{11,00}$, where $A_{v'J',vJ}$ stands for the spontaneous decay rate from an upper level (v', J') to a lower level (v, J). For the relevant cases $T \leq 300$ K, this inequality is satisfied for most diatomics. Vibrational blackbody excitation and deexcitation is taken into account for all levels considered. It is negligible in $HD^+$ at room temperature compared to competing rates, but more generally may become relevant for the (0,0) ground state, since the blackbody excitation rate $\Gamma_{00,11}(T)$ for (0, 0) → (1, 1) can become comparable or larger than the rotational blackbody rate $\Gamma_0(T)$ for (0, 0) → (0, 1) at more elevated temperatures.

The major simplification of the model is the way we account for the detailed hyperfine structure of the rovibrational states. If the frequency spectrum of a radiation field driving a transition is broad compared to the spectral width of the transition's hyperfine spectrum (typically < 150 MHz [Bakalov1]), the hyperfine absorption spectrum can be approximated by a single line with a spectral profile given by the envelope of the actual hyperfine spectrum. Since under typical experimental conditions the Doppler broadening of 10 - 20 MHz of the hyperfine lines is comparable to the typical separation of adjacent hyperfine lines, we approximate each hyperfine spectrum by a single gaussian absorption profile of appropriate width. For optical pumping to be efficient the lasers must have similar spectral widths as the respective transition spectra and sufficient spectral intensity to saturate the transitions.

## Maximum efficiency for two-laser rotational cooling

In steady-state, the rate equations reduce to algebraic equations, which may be solved analytically for the populations $p_J$, leading to in general very complicated expressions. In order to obtain a more simple yet reliable explicit analytical expression for the theoretically achievable ground state population $p_0$, we make a few reasonable approximations. Blackbody excitation and deexcitation is taken into account only within the v = 0 rotational levels and for the vibrational transitions (0, 0) ↔ (1, 1) and (0, 2) ↔ (1, 1). The neglect of other blackbody processes does not lead to a stronger condition on $h \nu_{rot}/k_B T$ than the above. Thus, among vibrationally excited states only the states (v = 1, J = 1), (v = 2, J = 0) excited by the two pump lasers are taken into

account. In v = 0 we consider the levels from J = 0 to $J_{max}$ = 8. Hyperfine structure is neglected. The overtone spontaneous decay (2,0) → (0,1) is not explicitly included, since typically $A_{20,01}/A_{20,11} << 1$ and its effect can, if necessary, be accounted for by a rescaling of the pump intensity for that transition.

For simplicity, the diatomic molecule is approximated as a rigid rotor, whose (v = 0, J) rotational level energies are given by J(J+1) h $\nu_{rot}$/2 and whose rotational transition matrix elements $M_{JJ'}$ are all set equal, $M_{JJ'} = M_{01}$. These two approximations are well satisfied for molecular species with large $\nu_{vib}$ and do not impact the applicability of the result below. This leaves four independent spontaneous emission rates that are taken into account, the fundamental rotational spontaneous rate $A_{01,00}$ and the vibrational rates $A_{11,00}$, $A_{11,02}$, $A_{20,11}$. The ratio of blackbody-induced vibrational excitation rate from the ground state, $\Gamma_{00,11}(T)$, and the rotational excitation, $\Gamma_0(T)$, is denoted by $\gamma$.

The population fraction not in the ground state decreases with increasing pump intensities and the lowest value is found in the limit of intensities much larger than the saturation intensities. This regime is achievable experimentally. The asymptotic value of $p_0$ is independent of the intensities, and is given, to a good approximation, by

$$1 - p_0(T) = \left(\frac{A_{01,00}}{A_{20,11}}\right) \frac{12 + (1+\gamma)FA_{20,11}/A_{11,00}}{1 - \xi + (A_{01,00}/A_{20,11})(G + (F + \gamma F + \gamma)\xi A_{20,11}/A_{11,00})}\,\xi \qquad (1)$$

The value $p_0$ is temperature-dependent via the functions $\xi(T) = \exp(-h\,\nu_{rot}/k_B\,T)$, $F(T) = 5 + 7\,\xi^3 + 9\,\xi^7 + 11\,\xi^{12} + 13\,\xi^{18} + 15\,\xi^{25} + 17\,\xi^{33}$, $G(T) = 3\,(1 + 5\,\xi + 20\,\xi^2)/(1+\xi)$, and $\gamma(T) = (\exp(h\nu_{rot}/k_BT) - 1)A_{11,00}\,/((\exp(h\nu_{vib}/k_BT) - 1)A_{01,00})$. The ratios of spontaneous emission rates appearing in Eq. (1) are $A_{20,11}/A_{11,00}$, of order 6, and the ratio of a rotational spontaneous rate and a Δv = 1 vibrational spontaneous rate, $\alpha_{r2} = A_{01,00}/A_{20,11} << 1$. Eq.(1) is applicable if $\xi^9 << 1$ and as long as the result is << 1, i.e. the individual populations in rotational levels other than (0, 0) are low (< 0.1), so that the limitation of the number of excited rotational levels ($J_{max}$) taken into account in v = 0 is adequate.

A simple interpretation of equation (1), neglecting the third (~ $\alpha_{r2}$) term in the denominator, is as follows. The ground state population is given by the equilibrium between the black-body induced excitation (0, 0) → (0, 1) from the ground state with rate $\Gamma_0(T) = 3\,\xi\,A_{01,00}\,/(1-\xi)$, and the repopulation of the ground state by the pump fields. The latter process starts from excited rotational levels and proceeds by channels that involve both the spontaneous emission (2, 0)→ (1, 1) and (1, 1) → (0, 0) and is thus given by (1 - $p_0$) times a weighted combination of the rates $A_{11,00}$ and $A_{20,11}$.

Eq.(1) permits to evaluate if the two-laser scheme is efficient for a given heteronuclear diatomic molecule at a given temperature T of the blackbody radiation field. Sufficient conditions are h $\nu_{rot}/(k_B\,T) >> F(T)A_{01,00}/A_{11,00}$ and h $\nu_{vib}/(k_B\,T) > \ln(F(T)) + 3$, i.e. both a sufficiently low

rotational frequency (since $A_{01,00} \sim \nu_{rot}^3$), and a sufficiently high vibrational frequency. For a given molecular species, these conditions can be satisfied if the blackbody temperature is sufficiently low. For an environment at room temperature and for many heteronuclear ion species, this is the case. Moderate cooling of the environment can further reduce the excited fraction.

With the notation $A_{vib} = A_{20,11}$, the proportionality $A_{11,00} \propto A_{vib}$, using the relationship between $\Gamma_0(T)$ and $A_{01,00}$, and considering molecules with large $\nu_{rot}$, (i.e. $\gamma << 1$) gives the scaling quoted in the main text.

For $HD^+$, the relevant molecular properties are $\nu_{vib} \cong 1955\ cm^{-1}$, $\nu_{rot} \cong 43.86\ cm^{-1}$, $A_{11,00} \cong 5.8\ s^{-1}$, $A_{11,02} \cong 12.3\ s^{-1}$, $A_{20,11} \cong 31.9\ s^{-1}$, $A_{01,00} \cong 6.7 \times 10^{-3}\ s^{-1}$, and thus $\alpha_{r2} \cong 2.1 \times 10^{-4}$, $\gamma(300\ K) \cong 0.02$.

At T = 300 K, Eq. (1) predicts $1 - p_0 = 7.8\%$ for the lowest achievable non-ground state population for very high intensities. The result without approximations, using the full set of rate equations described in the section "Rate equation model", is 8.0%. The values are 12% (8.9%), for intensities equal to 1 (5) times the respective saturation intensities,.

**Rotational state detection**

A continuous-wave (cw) UV-laser at 266 nm ($I_{UV} \cong 128\ mW/mm^2$) dissociates molecular ions in the v = 4 state via excitation to the 2pσ excited state without affecting ions in the v = 0 state. We can therefore selectively dissociate molecular ions from one specific (0, J) state by simultaneous excitation of a (0, J) → (4, J ± 1) transition with a broadly tunable cw diode laser (1370 -1480 nm, $I_{IR} \cong 19\ mW/mm^2$) that is spectrally broadened to 285 MHz FWHM. The resulting loss of $HD^+$ ions is detected by exciting resonantly the secular motion of the remaining $HD^+$ ions in the trap with an auxiliary rf field ($f_{rf} \cong 800$ kHz) for a time $t_s$. This leads to additional heating of the Coulomb crystal with a heating rate $\Gamma_N$ proportional to the number of HD ions in the trap N. The total heating rate is then $\Gamma_h = \Gamma_0 + \Gamma_N$, where $\Gamma_0 << \Gamma_N$ is an approximately constant heating rate independent of N. Far away from the Doppler-limit the laser cooling of the two-species Coulomb crystal can be described semi-classically in a similar way as for a single ion [Morigi1] and below saturation the cooling rate $\Gamma_c$ is to good approximation proportional to the $Be^+$ fluorescence rate $\Gamma_f$ [Wineland1]. In the steady state we have $\Gamma_f \sim \Gamma_0 + \Gamma_N$ with secular excitation and $\Gamma_f \sim \Gamma_0$ without. We measure $\Delta\Gamma \sim \Gamma_f - \Gamma_0 \sim \Gamma_N$ for a fixed amplitude of the secular excitation field before ($\Delta\Gamma_1$) and after ($\Delta\Gamma_2$) applying the REMPD lasers for a time $t_d$ (see Fig. 3). Since we work with the $Be^+$ cooling laser frequency set to about 0.7 atomic linewidth below resonance, the fluorescence rate increases when the temperature of the ion ensemble increases. We define our detection signal $S_J$ as

$$S_J = \frac{\langle \Delta\Gamma_1 \rangle - \langle \Delta\Gamma_2 \rangle}{\langle \Delta\Gamma_1 \rangle} = 1 - \frac{N_2}{N_1} \tag{2}$$

where the average is taken over the time $t_s$ and $N_1$ ($N_2$) is the initial (final) total number of $HD^+$ ions in the trap. If the detection time is small compared to the blackbody thermalization time and spontaneous decay from the (4, J ± 1) state prior to dissociation can be neglected, the relative population $p_J$ in the state (0, J) is $p_J = S_J - S_b$, where $S_b$ is the background relative loss of $HD^+$ ions if the REMPD lasers are off during $t_d$.

**References**


[1] Crompvoets, F. M. H., Bethlem, H. L., Jongma, R. T., and Meijer, G. A prototype storage ring for neutral molecules, Nature 411, 174 (2001).

[2] Rieger, T., Junglen, T., Rangwala, S. A., Pinkse, P. W. H., and Rempe, G. Continuous loading of an electrostatic trap for polar molecules. Phys. Rev. Lett. 95, 173002 (2005).

[3] Campbell, W. C., Doyle, J. M., and references therein. In: Cold Molecules, Krems, R. V., Stwalley, W. C., and Friedrich, B., editors, *Cold Molecules*, p. 473. (CRC Press, Boca Raton, 2009).

[4] A. Fioretti et al., Formation of cold $Cs_2$ molecules through Photoassociation. Phys.Rev.Lett. 80, 4402 (1998).

[5] E. Hodby et al. Production efficiency of ultracold Feshbach molecules in bosonic and fermionic systems. Phys. Rev. Lett. 94, 120402 (2005).

[6] S. Jochim et al. Bose-Einstein condensation of molecules. Science 302, 2101 (2003).

[7] Regal, C. A., Ticknor, C., Bohn, J. L., and Jin, D. S. Creation of ultracold molecules from a Fermi gas of atoms. Nature 424, 47 (2003).

[8] Weinstein, J. D., deCarvalho, R., Guilett, T., Friedrich, B., and Doyle, J. D. Magnetic trapping of calcium monohydride molecules at millikelvin temperatures. Nature 395, 148 (1998).

[9] Mølhave, K. and Drewsen, M. Formation of translationally cold $MgH_{¿}$ and $MgD_{¿}$ molecules in an ion trap, Phys. Rev. A 62 011401(R)

[10] Roth, B., Koelemeij, J. C. J., Daerr, H., and Schiller, S. Rovibrational spectroscopy of trapped molecular hydrogen ions at millikelvin temperatures. Phys.Rev.A 74, 040501(R) (2006).

[11] Ostendorf, A., Zhang, C., Wilson, A., Offenberg, D., Roth, B., and Schiller, S., Sympathetic cooling of complex molecular ions to milli-Kelvin temperatures, Phys. Rev. Lett. 97, 243005 (2006)

[12] J. G. Danzl et al. Quantum gas of deeply bound ground state molecules. Science 321, 1062 (2008).

[13] J. Deiglmayr et al. Formation of ultracold polar molecules in the rovibrational ground state. Phys.Rev.Lett. 101, 133004 (2008).

[14] Lang, F., Winkler, K., Strauss, C., Grimm, R., and Denschlag, J. H. Ultracold triplet molecules in the rovibrational ground state. Phys.Rev.Lett. 101, 133005 (2008).

[15] K. -K. Ni et al. A high phase-space-density gas of polar molecules. Science 322, 231 (2009).

[16] DeMille, D. Quantum computation with trapped polar molecules, Phys. Rev. Lett. 88, 067901 (2002)

[17] Schiller, S. and V. Korobov, V., Tests of time independence of the electron and nuclear masses with ultracold molecules, Phys. Rev. A 71, 032505 (2005)

[18] Koelemeij, J. C. J., Roth, B., Wicht, A., Ernsting, I., and Schiller, S., Vibrational Spectroscopy of $HD^+$ with 2-ppb accuracy, Phys.Rev.Lett. 98, 173002 (2007).

[19] Krems, R. V., Stwalley, W. C., and Friedrich, B., editors, *Cold Molecules*, (CRC Press, Boca Raton, 2009).

[20] Morigi, G., Pinkse, P. W. H., Kowalewski, M., and de~Vivie-Riedle, R. Cavity cooling of internal molecular motion. Phys.Rev.Lett. 99, 073001 (2007).

[21] Hudson, E. R. Method for producing ultracold molecular ions. Phys.Rev.A 79, 032716 (2009).

[22] Vogelius, I. S., Madsen, L. B., and Drewsen, M. Blackbody-radiation–assisted laser cooling of molecular ions. Phys.Rev.Lett. 89, 173003 (2002).

[23] Højbjerre, K., Hansen, A. K., Skyt, P. S., Staanum, P. F., and Drewsen, M. Rotational state resolved photodissociation spectroscopy of translationally and vibrationally cold $MgH^+$ ions: toward rotational cooling of molecular ions. New J. Phys. 11, 055026 (2009).

[24] Koelemeij, J. C. J., Roth, B., and Schiller, S. Blackbody thermometry with cold molecular ions and application to ion-based frequency standards. Phys.Rev.A 76, 023413 (2007).

[25] Vogelius, I. S., Madsen, L. B., and Drewsen, M. Rotational cooling of heteronuclear molecular ions with $^1\Sigma$, $^2\Sigma$, $\Sigma$, and $^1\Pi$ electronic ground states. Phys.Rev.A 70, 053412 (2004).

[26] Korobov, V. I. Leading-order relativistic and radiative corrections to the rovibrational spectrum of $H_2^+$ and $HD^+$. Phys.Rev.A 74, 052506 (2006).

[27] Colbourn, E. A. and Bunker, P. R. Accurate theoretical vibration-rotation energies and transition moments for $HD^+$, $HT^+$, and $DT^+$. J.Mol.Spect. 63, 155 (1976).

[28] Bakalov, D., Korobov, V. I., and Schiller, S. High-precision calculation of the hyperfine structure of the $HD^+$ Ion. Phys.Rev.Lett. 97, 243001 (2006).

[29] Morigi, G. and Eschner, J. Doppler cooling of a Coulomb crystal. Phys.Rev.A 64, 063407 (2001).

[30] Wineland, D. J. and Itano, W. M. Laser cooling of atoms. Phys.Rev.A 20, 1521 (1979).

## Acknowledgements

The authors thank M. Hansen, S. Vasilyev, E. Zlobina for contributions to the experimental setup and A. Nevsky for helpful discussions. This work is supported by the Deutsche Forschungsgemeinschaft under grant SCHI 431/11-1.

## Competing Financial Interests statement

The authors declare no competing financial interests.

## Author contributions

T.S. and B.R. planned and performed the experiments, S.S. and H.D. participated,
T.S. performed data evaluation, numerical simulations, B.R. participated,
S.S. and H.D. developed the QCL and DFB laser system,
S.S. conceived the study, developed the rate equation model and analytic treatment,
I.E. developed a near-infrared diode laser system and participated in preliminary and complementary investigations;
T.S. wrote the paper, B.R. and S.S. participated.

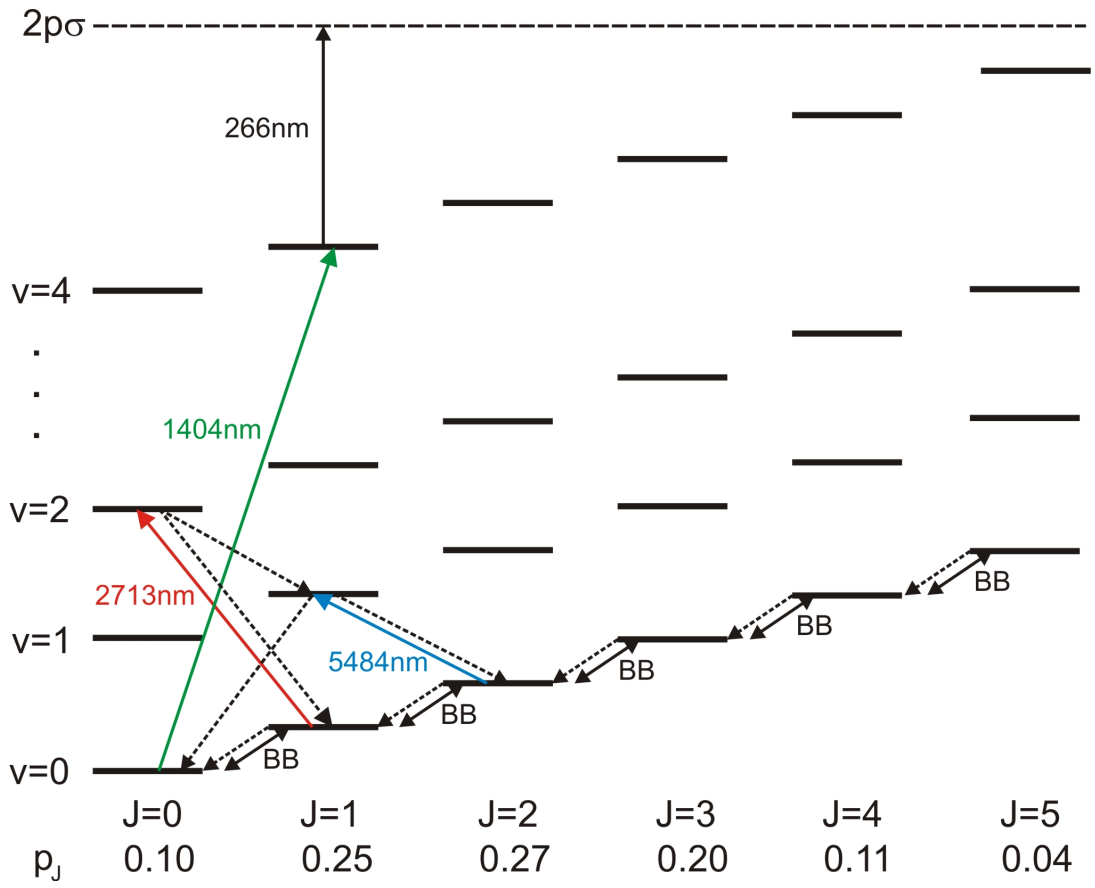


Figure 1

Schematic view of relevant rovibrational states and dipole transitions in the 1sσ electronic ground state of $HD^+$ (not to scale). 5484 nm and 2713 nm transitions: optical pumping. 266 nm and 1404 nm transitions: state selective detection by (1+1)-photon dissociation. BB: blackbody radiation. Dashed lines: dipole spontaneous decay channels. $p_J$: fractional rotational state populations in v = 0 at T = 300 K.

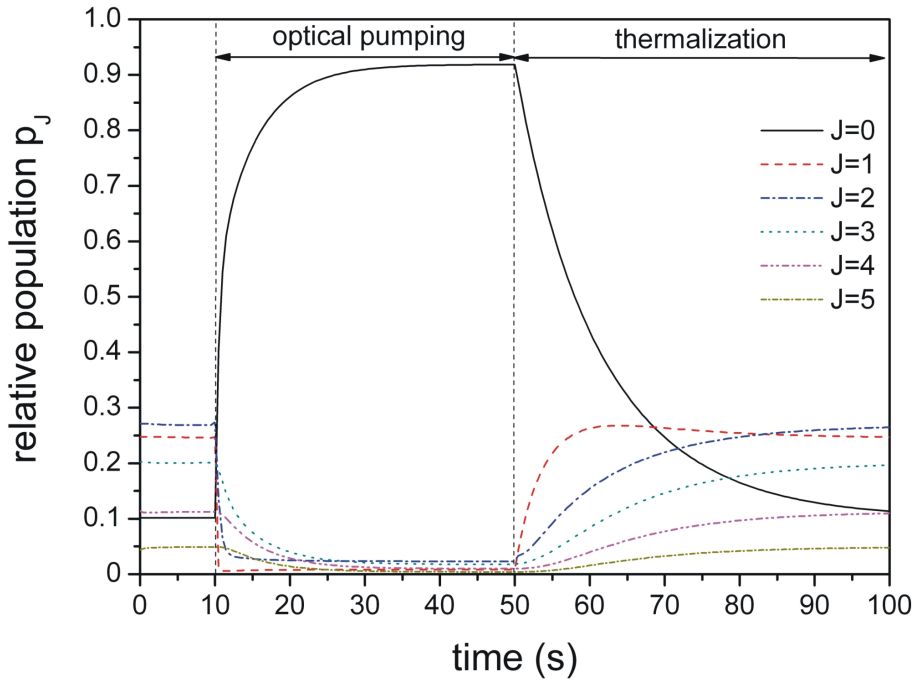


Figure 2

Rate equation simulation for the dynamics of the rotational state distribution in the vibrational ground state. Shown is the time evolution for simultaneous optical pumping on the (0, 1)→(2, 0) and (0, 2) → (1, 1) transitions as well as thermalization with the T = 300 K blackbody radiation after the optical pumping fields have been turned off.

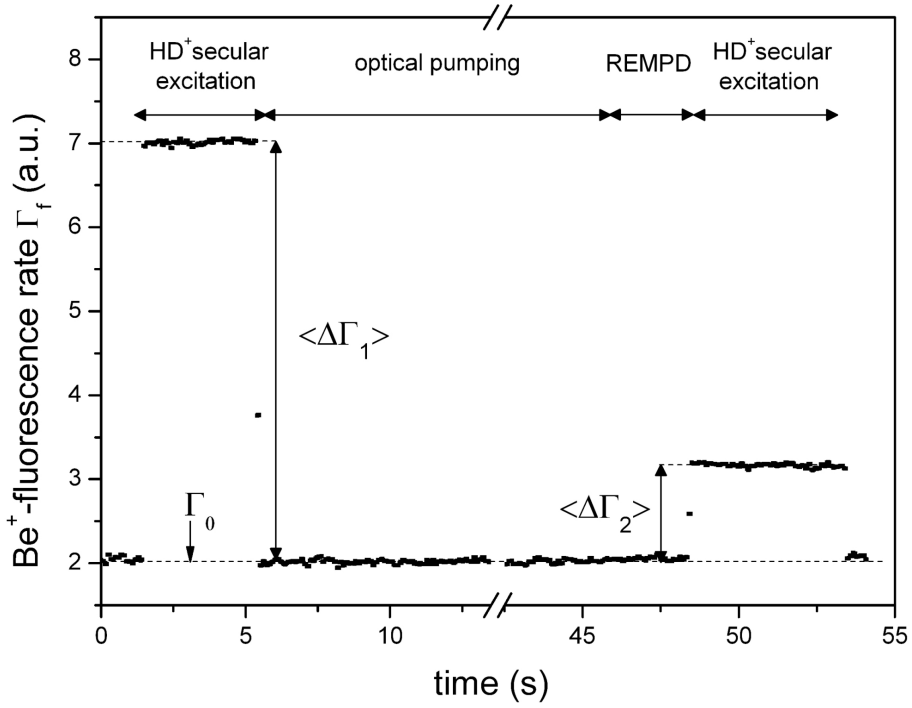


Figure 3

Experimental sequence for determining the population $p_J$ in the state (v=0, J) and typical experimental REMPD data for J = 0. $<\Delta\Gamma_1>$ ($<\Delta\Gamma_2>$) is the average change in the $Be^+$ fluorescence during the first (second) secular excitation.

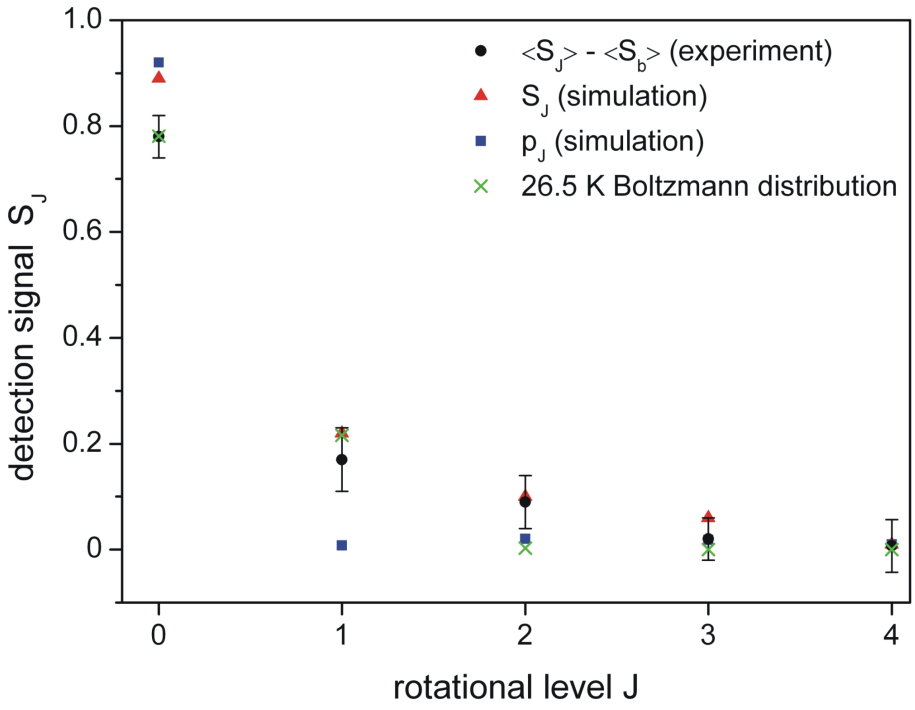


Figure 4

Rotational state distribution of the vibrational ground state after applying the optical pumping scheme. Black dots: mean background corrected detection signals $\langle S_J \rangle - \langle S_b \rangle$. Error bars represent the 1σ standard deviation of the sample. Red triangles: Detection signals predicted by rate equation simulations for the experimental parameters. Blue squares: relative state populations $p_J$ predicted by rate equation simulations for the experimental parameters. Green crosses: Boltzmann distribution for T = 26.5 K.